Faraday Discussions

Cite this: *Faraday Discuss.*, 2014, **174**, 357



# Novel electrochemiluminescent materials for sensor applications†

Lynn Dennany,* Zahera Mohsan, Alexander L. Kanibolotsky and Peter J. Skabara

Received 2nd May 2014, Accepted 19th June 2014
DOI: 10.1039/c4fd00090k

Electrochemiluminescence (ECL) uses redox reactions to generate light at an electrode surface, and is gaining increasing attention for biosensor development due to its high sensitivity and excellent signal-to-noise ratio. ECL studies of monodisperse oligofluorene–truxenes (T4 series) have been reported previously, showing the production of stable radical cations and radical anions, generating blue ECL. The compound in this study differs from the original structures, in that there are 2,1,3-benzothiadazole (BT) units inserted between the first and second fluorene units of the quarterfluorenyl arms. It was therefore anticipated that the incorporation of these highly luminescent and ECL-active compounds into sensor development would lead to significant decreases in detection limits. In this contribution, we report on the impact of incorporating these novel complexes into sensor devices on the ECL efficiency, as well as the ability of these to improve the detection sensitivity and decrease the limit of detection using the reagent-free detection of model analytes. The real world impact of these compounds is elucidated through the comparison with more standard ECL materials such as ruthenium-based compounds. The potential for multiple applications is to be examined within this contribution.

## Introduction

Electrochemiluminescence (ECL) represents a powerful analytical approach that combines simple equipment with inherent sensitivity, and a wide dynamic range for many analytes.[1,2,3,4,5] ECL has been the subject of extensive study for the past three decades.[6–8] The production of light from intermediates generated during electrolysis occurs when the energy liberated by the reaction between the electrogenerated precursors is sufficient to generate a product in an electronically excited form.[9] Studies of inorganic ECL have been dominated by transition metal complexes,[10–12] particularly ruthenium poly(pyridyl) species, *e.g.*, those of the general formula $Ru(L)_3^{2+}$, where L = 2,2′-bipyridine,[13–15] 4,7-diphenyl-1,10-

*WestCHEM, Department of Pure and Applied Chemistry, University of Strathclyde, 295 Cathedral Street, Glasgow, G1 1XL, UK. E-mail: lynn.dennany@strath.ac.uk; Fax: +141 548 2535; Tel: +141 548 4322*

† Electronic supplementary information (ESI) available. See DOI: 10.1039/c4fd00090k

phenanthroline[16] or 2,2′-bipyrazine.[17] This is due to the attractive photophysical and electrochemical properties that these compounds typically exhibit. ECL is a remarkably versatile, highly sensitive[18] and selective technique that has emerged in various research fields.[19] In recent years, particularly fascinating electronic properties have been discovered for various star-shaped conjugated oligomers with different core arms.[20]

As with all sensors, there is a constant drive to improve their sensitivity and selectivity. The future health industry in conjunction with point of care health monitoring will demand the detection of life-threatening diseases before critical stages have been reached. This will require a new breed of biomedical sensors capable of measuring disease biomarkers down to the picomolar range. In order to design such sensors, it is necessary to consider the limitations of the current biomedical sensors.

Depending on the nature of a specific ECL reaction, the sensitivity of ECL-based systems may be limited by certain factors. These include slow rates of charge transfer ($D$). A slow rate of diffusion will lead to slow regeneration of the excited state, typically $Ru^{3+}$, which is required to react with an analyte to produce ECL. A fast diffusion rate to the electrode will lead to an increase in the amount of the excited state available to react with a specific analyte. This should lead to increased ECL production and improved sensitivity. One appealing possibility is to wire the luminophores using a conjugated polymer backbone which can have a positive effect on ECL efficiencies.[21] An alternative to this is to create an entirely new compound with high luminescence quantum yields to allow for the determination of lower concentrations of the target analyte.

ECL can be produced by two dominant pathways, *i.e.* annihilation and co-reactant pathways.[8] The co-reactant pathway is predominantly utilised for sensor applications, and the common oxidation mechanism for inorganic compounds corresponding to the production of ECL through the interaction of an ECL-active material with a co-reactant is well established, and is as follows:[2,4,5,7,8]

$$ML^{n+} \rightarrow ML^{n+1} + e^- \quad (1)$$

$$ML^{n+1} + \text{analyte} \rightarrow ML^{n+} + \text{analyte}_{Ox} \quad (2)$$

$$\text{Analyte}_{Ox} \rightarrow \text{analyte}_{Med.Ox} + \text{analyte}_{radical} \quad (3)$$

$$\text{Analyte}_{radical} + ML^{n+} \rightarrow \text{analyte}_{Med.Ox} + ML^{n+}* \quad (4)$$

$$ML^{n+}* \rightarrow ML^{n+} + h\nu \quad (5)$$

where ML is the ECL-active material and the analyte can refer to either the target compound being analysed or the co-reactant undergoing mediated oxidation, thereby producing an ECL response. The ECL produced is often governed by the concentration of the excited state form of the ECL-active material, usually determined in the solution phase by the diffusional coefficient observed.

This work will examine the applicability of star-shaped conjugated oligomers, specifically truxene–oligofluorene with 2,1,3-benzothiadazole units (T4BT–B), to facilitate future ECL sensor development. This system will be compared to a common ECL system, namely utilising $[Ru(bpy)_3]^{2+}$ for the determination of tri-propylamine (TPA) concentrations. TPA is often used as a co-reactant for ECL

 

production and by comparing the ECL response of T4BT–B with that of $[Ru(bpp)_3]^{2+}$ to TPA, we will evaluate the ECL production and efficiency of T4BT–B. Many clinically relevant biomarkers are detected through the co-reactant pathway and many are based upon the interaction of amine structures. Therefore, TPA is being utilised as a model for how other proteins would interact with T4BT–B. In addition, there are a considerable number of illicit substances which also have amine-based structures, and T4BT–B could also be utilised for their detection following the same reaction pathways as shown for TPA. Electrochemical sensors are not entirely focused on amine detection, but ECL sensors are particularly prevalent in biosensor applications and can also be utilised as co-reactants for label-based ECL systems.[2,4,5,7,8] Since TPA represents a particularly well-established system, both for biosystems detection and label-based ECL systems, it was utilised as a model system to be investigated in this study.

# Experimental section

### Materials and reagents

The star-shaped truxene compound with additional 2,1,3-benzothiadiazole units (T4BT–B, shown in Fig. 1) has been synthesised as previously described.[22–25] $[Ru(bpy)_3]^{2+}$ was purchased from Sigma Aldrich and utilised without purification.

All solvents used were of spectroscopic grade. The working electrodes were prepared by polishing with alumina (1.0–0.3 μm) on a felt pad. All solutions were deoxygenated using nitrogen or argon prior to measurement.

### Apparatus

Electrochemical experiments were performed in a standard electrochemical cell using a CH instruments (Memphis, TN) model 760D potentiostat. Cyclic voltammetry experiments were carried out using a 3 mm diameter glassy carbon working electrode in a conventional three electrode assembly using a platinum flag as the counter electrode and an Ag wire as the reference electrode. Potentials were controlled *versus* a standard Ag wire reference electrode. Measurements

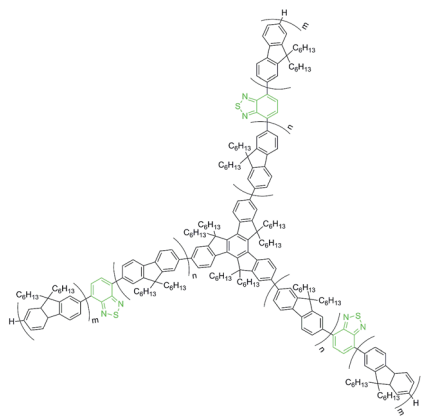

Fig. 1 Chemical structure of truxene–quarterfluorenes with BT (green) units, $n = 1$, $m = 3$ for T4BT–B.

involving simultaneous detection of light and current utilised a CH instrument model 760D connected to a Hamamatsu (H6780-20) photomultiplier tube (PMT). The PMT was biased at −800 or −400 V (indicated where utilised) by a high voltage power supply. During the experiments, the cell was kept in a light-tight box in a specially designed holder where the working electrode was positioned directly opposite to the fibre optic bundle, the other end of which was coupled to the PMT.

All measurements were made at room temperature (20 °C). For ECL experiments, concentrations of up to 2 mM tripropylamine (pH 6) were used as the co-reactant. For a comparison of ECL systems, $1 \times 10^{-4}$ M solutions of T4BT–B in anhydrous dichloromethane ($CH_2Cl_2$) and separate solutions of $1 \times 10^{-4}$ M $[Ru(bpy)_3]^{2+}$ in 0.1 M tetrabutylammonium hexafluorophosphate ($(TBA)PF_6$) in anhydrous dichloromethane ($CH_2Cl_2$) electrolyte with varying concentrations of TPA were used. All other reagents used were of analytical grade.

## Results and discussion

### Electrochemical properties of T4BT–B

The electrochemical behaviour of the T4BT–B compound and $[Ru(bpy)_3]^{2+}$ were examined using cyclic voltammetry. Fig. 2 shows the typical voltammetric behaviour of both compounds. By analogy with the voltammetric behaviour of $Ru^{2+/3+}$ complexes,[2,4,7,14] the peaks centred at $\sim E_{1/2} = 1.2$ V are attributed to the $Ru^{2+/3+}$ couple while those at −1.44 and −1.64 V are bpy-based reductions to the +1 and 0-charged species respectively. In addition, the peak-to-peak separation between the anodic and cathodic waves is close to zero at low scan rates, the full width at half maximum (FWHM) is close to the theoretically value of 59 mV, and the peak current varies linearly with the square root of the scan rate.

Fig. 2 also shows the voltammetric behaviour of T4BT–B, consisting of three overlapping anodic waves. The peak-to-peak separation of this first anodic wave is close to zero, as anticipated. This first anodic wave is fully reversible, followed by two quasi-reversible waves. The reduction of T4BT–B shows a stable single

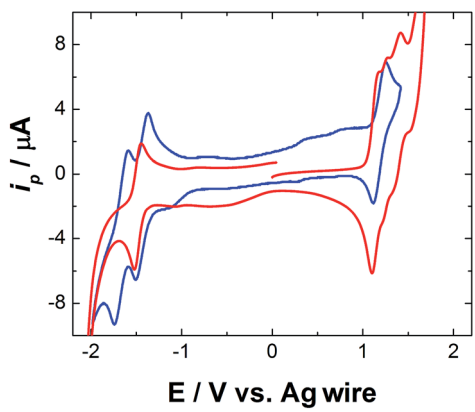


Fig. 2 Solution phase cyclic voltammetric behaviour of $1 \times 10^{-4}$ M T4BT–B (red line) and $1 \times 10^{-4}$ M $[Ru(bpy)_3]^{2+}$ (blue line). The electrolyte was 0.1 M $(TBA)PF_6$ in $CH_2Cl_2$, and a scan rate of 100 mV $s^{-1}$ was used.

reversible cathodic wave at ~−1.49 V. For each of these compounds, the peak current increases linearly with the square root of the scan rate for both the oxidation and reduction processes. However, given the overlapping anodic waves, the FWHM cannot be determined. This behavior is consistent with semi-infinite linear diffusion limiting the redox process, and under these conditions the response can be described by the Randles–Sevçik equation:

$$i_p = 0.4463nFAC\left(\frac{nF\nu D}{RT}\right)^{\frac{1}{2}} \quad (6)$$

where $n$ is the number of electrons transferred, $A$ is the area of the working electrode, $\nu$ is the scan rate, $D$ is the diffusion coefficient, $F$ is the Faraday constant, $R$ is the gas constant, $T$ is the temperature in Kelvin, and $C$ is the concentration of the redox centers. Thus, eqn (6) allows $D$ to be estimated for both the oxidation and reduction processes of each compound, provided that $n$ is known (or assuming a value for $n$; for T4BT–B in DCM an $n$ value of 1 is assumed). Table 1 shows the $D$ values for the oxidation process for T4BT–B and $[Ru(bpy)_3]^{2+}$.

ECL production can be highly dependent upon the rate of generation of the excited state, which is often based on the diffusion coefficient ($D$) that is calculated for the ECL-active species. The faster the diffusion coefficient, the more $ML^{n+1}$ is available for interaction with the co-reactant or analyte of interest, thereby producing an ECL response. A slower diffusional rate and insufficient amounts of $ML^{n+1}$ will result in decreased ECL emission and hence decreased sensitivity. A faster diffusion rate would thereby significantly increase the production of ECL, leading to enhanced sensitivity. This increase coupled with an increased luminescence yield should lead to favourable characteristics necessary for enhanced ECL production. The diffusion coefficients for $[Ru(bpy)_3]^{2+}$ and T4BT–B are given in Table 1. Different solvents are utilised for this comparison, with the optimal conditions for each material being utilised and therefore facilitating comparison of the most efficient systems for ECL production.

This slightly faster regeneration diffusion coefficient of T4BT–B may ultimately increase the efficiency of an ECL system based on this star-shaped compound. This could impact greatly on sensor design, as the faster regeneration of the excited state species should drastically improve the sensitivity of systems involving these star-shaped compounds; although other factors may also have an influence, the diffusion rates are a factor solely influenced by the properties of the material itself. These values were calculated using cyclic voltammetry and will be confirmed in future work by investigation using chronoamperometry. Both the influence of the rate of reaction and diffusion rates of the electrogenerated

**Table 1** $D$ for $1 \times 10^{-4}$ M T4BT–B in DCM and $1 \times 10^{-4}$ M $[Ru(bpy)_3]^{2+}$ in 0.1 M $(TBA)PF_6$ in $CH_2Cl_2$, based on the results from Fig. 2[a]

| Compound | $D \pm 0.08$ ($cm^2\ s^{-1}$) |
|---|---|
| $[Ru(bpy)_3]^{2+}$ | $2.3 \times 10^{-6}$ |
| T4BT–B | $1.63 \times 10^{-5}$ |

[a] All values are based on averaged results from 3 independent measurements.

product will impact on the efficiency of ECL production. To contrast the efficiency of the materials themselves, the diffusion coefficient can be an important parameter to investigate when examining the potential of ECL-generating materials.

### Electrochemiluminescence properties

One of the key objectives of this work was to investigate whether T4BT–B exhibits ECL in comparative dynamic linear ranges compared to ruthenium-based systems and to subsequently compare the efficiency of ECL generation of these two systems for the detection of TPA. Fig. 7 shows the potential dependence of the ECL response for both T4BT–B and $[Ru(bpy)_3]^{2+}$ using TPA as the co-reactant. Both systems produced ECL upon electrochemical production of the cation radicals $T4BT–B^{+}$ and $[Ru(bpy)_3]^{3+}$ respectively, in the presence of TPA. However, these intensities were considerably higher for the T4BT–B system in comparison to the $[Ru(bpy)_3]^{2+}$-based system under the same experimental conditions.

For the detection of amino acids, specifically TPA in this study, the electrogenerated $[Ru(bpy)_3]^{3+}$ has been shown to undergo a mediated oxidation reaction with the amino acids. Significantly, the chemiluminescence intensity is maximised at pH values near the $pK_a$ of the N-terminal amine site.[2] The T4BT–B compound undergoes a similar process with the reaction between the electrogenerated $T4BT–B^{+}$ and the TPA being sufficiently energetic to produce an ECL response. Direct oxidation of TPA occurs at ~2.1 V. As with the reaction mechanism for ruthenium, T4BT–B and TPA are simultaneously oxidised during a single potential step to produce $(T4BT–B)^{+\cdot}$ and $TPA^{+}$ respectively. The TPA radical then loses a proton to form the strongly reducing radical species $TPA^{\cdot}$, which reacts with the $(T4BT–B)^{+\cdot}$, producing the excited state that emits light, according to eqn (7)–(11), which is similar to the mediated oxidation of oxalate by TPA.[26] This is a proposed scheme for the production of ECL from this new material, T4BT–B, and current investigations are ongoing to establish an exact mechanism.

$$T4BT–B - e^{-} \rightarrow (T4BT–B)^{+\cdot} \quad (7)$$

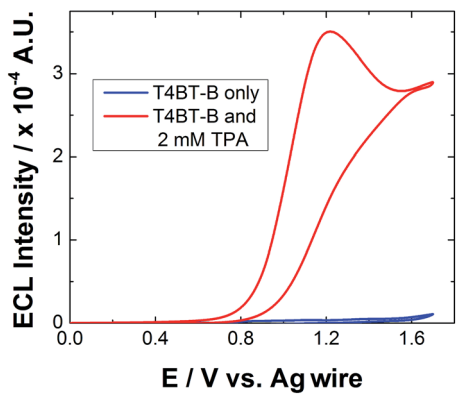


Fig. 3 Potential dependence of the ECL emission intensity of $1 \times 10^{-4}$ M T4BT–B in the presence (red line) and absence (blue line) of 2 mM TPA, monitored at a scan rate of 100 mV $s^{-1}$. The electrolyte was 0.1 M $(TBA)PF_6$ in anhydrous DCM.

 

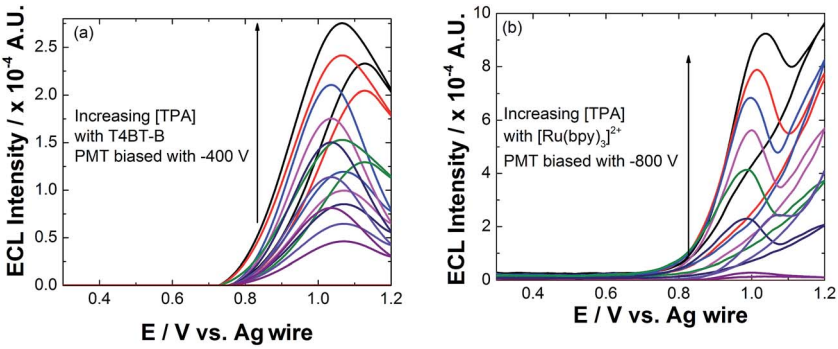


Fig. 4 ECL response of $1 \times 10^{-4}$ M (a) T4BT–B and (b) $[Ru(bpy)_3]^{2+}$ on the concentration of [TPA] at a scan rate of 100 mV $s^{-1}$ over the potential range 0.2 V $\leq E \leq$ 1.2 V *vs.* Ag wire. The PMT was biased at −400 V for (a) and −800 V for (b).

$$TPA - e^- \rightarrow TPA^{+} \quad (8)$$

$$TPA^{+} - H^{+} \rightarrow TPA^{\cdot} \quad (9)$$

$$(T4BT\text{–}B)^{+} + TPA^{\cdot} \rightarrow (T4BT\text{–}B)^{*} + Pr_2N^{+} = CHEt \quad (10)$$

$$(T4BT\text{–}B)^{*} \rightarrow T4BT\text{–}B + h\nu \quad (11)$$

Fig. 3 shows the potential dependence of the ECL emission intensity of T4BT–B. In the absence of TPA, there is no ECL response. However, in the presence of 2 mM TPA, the onset of light emission coincides closely with the onset of the oxidative current where the potential of T4BT–$B^{+}$ is generated, as can be seen in the inset of Fig. 7. This behaviour is consistent with TPA reducing the electro-generated T4BT–$B^{+}$ and creating the excited state species which subsequently results in the generation of ECL emission. The ECL emission intensity is centred

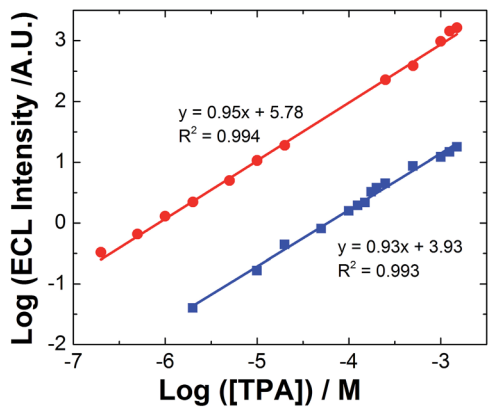


Fig. 5 Typical calibration plot of the dependence of the logarithm of the maximum ECL intensity on log[TPA] response for $1 \times 10^{-4}$ M T4BT–B (red line) and $[Ru(bpy)_3]^{2+}$ (blue line). The responses for T4BT–B have been adjusted for changes in the PMT bias.

at 564 nm, which is slightly shifted compared to the luminescence intensity which is centred at 551 nm (see ESI, Table S1 and Fig. S1†). In comparison to other T4 compounds,[20] where there was no fluorescence or ECL observed above 450 nm, for T4BT–B there was luminescence observed even above 550 nm, which can be related to the addition of BT units, attributing to longer wavelength emission. However, the ECL monitored is total light produced rather than monitoring a specific wavelength. Therefore, the advantages of a different wavelength of ECL emission are only assessed for systems of coloured matrices, and therefore it can be useful to have a variety of ECL emitters capable of producing ECL at a variety of different wavelengths.

The onset of the ECL emission is at approximately 0.8 V, which is significantly less positive than the standard redox potential of TPA of ~2.1 V.[2,27] This behaviour arises because a significant overpotential must be applied before TPA can be oxidised at a bare electrode. The large increase in emission intensity at circa 1.1 V clearly demonstrates that TPA is oxidised at potentials when the electrogenerated T4BT–B$^{+\bullet}$ sites exist, allowing interaction and subsequent ECL production to occur. This response can also be seen in the current response recorded simultaneously. Fig. 4 shows that the ECL response increases with increasing concentrations of TPA over the concentration range $2 \times 10^{-8}$ M $\leq$ [TPA] $\leq 2.0 \times 10^{-3}$ M for T4BT–B and over the range 1 $10^{-4}$ M $\leq$ [TPA] $\leq 2.0 \times 10^{-3}$ M for $[Ru(bpy)_3]^{2+}$.

Fig. 4 highlights the fact that although both compounds produced an ECL response in the presence of TPA, the magnitude of the response was dramatically higher for T4BT–B compared with $[Ru(bpy)_3]^{2+}$. In fact, to record responses, the settings of the PMT needed to be doubled for $[Ru(bpy)_3]^{2+}$ compared to T4BT–B to obtain similar responses. This result is consistent with the higher diffusion rates of T4BT–B, as well as the enhanced luminescence properties. Fig. 5 illustrates a typical calibration plot for [TPA] ranging from 0.2 μM to 2 mM based on the data obtained from Fig. 4; this cannot be compared directly to Fig. 6 since different PMT parameters were utilised. However, it does highlight the enhanced response

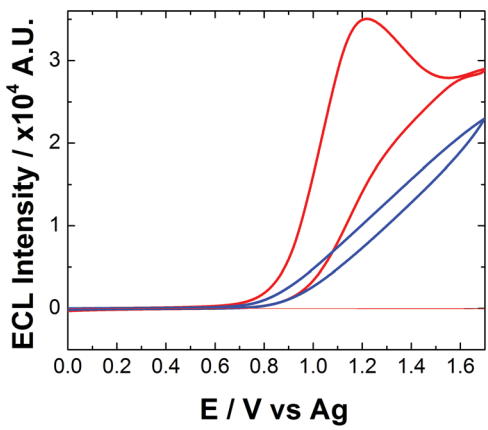


Fig. 6 ECL response of $1 \times 10^{-4}$ M T4BT–B only (red line) and with $2 \times 10^{-8}$ M TPA (blue line) at a scan rate of 100 mV s$^{-1}$ over the potential range 0 V $\leq \nu \leq$ 1.2 V *vs.* $Ag^+$. The PMT was biased at −750 V.

 

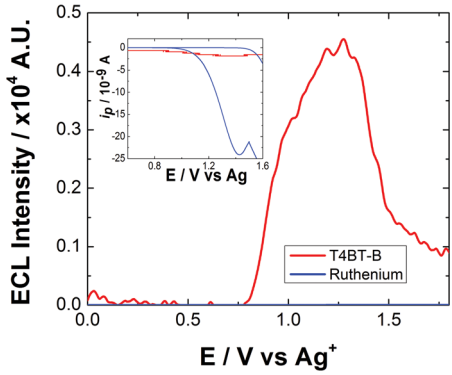


Fig. 7 Potential dependence of the ECL emission intensity of $1 \times 10^{-4}$ M T4BT–B (red line) and $1 \times 10^{-4}$ M $[Ru(bpy)_3]^{2+}$ (blue line) in the presence of 2 mM TPA, monitored at a scan rate of 100 mV $s^{-1}$. The electrolyte was 0.1 M $(TBA)PF_6$ in anhydrous DCM. The PMT was biased at −750 V. The inset shows the amperometric response recorded simultaneously.

for TPA when using the T4BT–B system. For each concentration, a well-defined response is observed with a high signal-to-noise ratio even at 20 pM, as can be seen in Fig. 7. This calibration plot demonstrates that $\log(I_{ECL})$ depends linearly on log[TPA] for both compounds. The logarithm of ECL intensity is almost directly proportional to log[TPA] (slope of 0.95), suggesting that although the TPA concentration does influence the light emission, other factors such as the diffusion of both species to the electrode do not play a major role in this system. The wide dynamic range and high S/N ratio makes T4BT–B attractive for reagent-free, ultrasensitive detection of chemical and biological analytes.

In terms of developing sensors, a key issue is the relative quantum efficiency of the materials. To evaluate this parameter, it is usual to compare the quantum efficiency of the new compound to a standard; for ECL production $[Ru(bpy)_3]^{2+}$ is most commonly used. The overall ECL efficiency ($\phi_{ECL}$) is defined as the number of photons emitted per Faradaic electron passed during the chemiluminescence reaction. It is a product of the efficiency of populating the excited state ($\phi_{EX}$) and the quantum yield of emission from the excited state ($\phi_P$), with $[Ru(bpy)_3]^{2+}$ normally used as the relative standard.[27] This investigation will be undertaken in future research, however, as an indication, the intensity of ECL produced under the same experimental conditions was examined to provide a quick insight into the efficiency of T4BT–B in comparison to $[Ru(bpy)_3]^{2+}$ utilising TPA as the co-reactant.

Although not as accurate as determining the $\phi_{ECL}$ for each system, Fig. 7 does highlight that the overall efficiency for T4BT–B would be higher than that obtained for $[Ru(bpy)_3]^{2+}$, which is usually taken as 5%.[2,4,28] Fig. 7 shows the response of both materials under identical conditions and can therefore be utilised for direct comparison. For T4BT–B a substantially lower current response is observed compared to that of the ruthenium system. Despite this, T4BT–B shows a dramatically higher ECL response. This also means that although T4BT–B has a slightly higher diffusion coefficient, it is more likely that the higher luminescence quantum yield (see Table S1†) is responsible for the greater ECL response. Fig. 6 shows that the ECL intensity obtained for T4BT–B is approximately twice that

observed for $[Ru(bpy)_3]^{2+}$. This enhanced efficiency is most likely due to a combination of the faster diffusion rates as well as the higher luminescence quantum yields (see ESI, Table S1 and Fig. S1†) of T4BT–B compared to $[Ru(bpy)_3]^{2+}$, and for these systems the higher luminescence quantum yields are most likely to contribute significantly more to the enhanced ECL. This is in conjunction with the limit of detection, LOD, defined as $I_{ECL.BLANK} + 3\sigma_{BLANK}$, which is 3 fM for the T4BT–B system, where $I_{ECL.BLANK}$ refers to the response when no co-reactant is added to the solution or noise inherent to the system and $\sigma$ refers to the standard deviation of this noise. This confirms that T4BT–B can enhance the ECL emission intensity. The wide dynamic range and low limit of detection makes T4BT–B attractive for biosensor and chemical sensor development. The additional benefits of lower power requirements for PMT settings due to the higher ECL intensity produced from equivalent concentrations of co-reactants also means that T4BT–B would be more viable for miniaturisation, which would be highly beneficial for biomedical, forensic and food monitoring applications.

# Conclusions

The electrochemical and ECL properties of the trigonal quarterfluorene–truxene oligomer with fused 2,1,3-benzothiadazole units, T4BT–B, have been presented here. T4BT–B shows good electrochemistry in $CH_2Cl_2$, with excellent stability properties of both the anion and cation radicals. T4BT–B also shows a yellow emission when generated by reaction with TPA, consistent with its photophysical properties. The production of ECL from the reaction of T4BT–B with TPA was shown to be linearly dependant over a wide dynamic linear range, with low limits of detection and good reproducibility, significantly producing almost double the ECL intensity compared to $[Ru(bpy)_3]^{2+}$ under the same experimental conditions. This work illustrates the proof of concept of the promising ECL sensing applications of this new family of compounds in a wide variety of applications ranging from biomedical diagnostics to forensic science. These possibilities are open due to the highly luminescent and fast charge transfer properties of these compounds which can be utilised to detect low levels of co-reactant without increasing the background noise levels, thereby allowing for the development of an ultrasensitive and selective ECL sensor.

# Acknowledgements

The authors acknowledge funding support from the Marie Curie Reintegration Grant (PIRG-2010-268236). PJS thanks the Royal Society for a Wolfson Research Merit Award.

# References

1 J. Li, S. Guo and E. Yang, *RSC Adv.*, 2012, **2**, 3579–3586.
2 L. Dennany, E. J. O'Reilly, T. E. Keyes and R. J. Forster, *Electrochem. Commun.*, 2006, **8**, 1588–1594.
3 H. Wei and E. Wang, *Chem. Soc. Rev.*, 2011, **26**, 77–85.
4 A. Devadoss, L. Dennany, C. Dickinson, T. Keyes and R. J. Forster, *Electrochem. Commun.*, 2012, **19**, 43–45.

5 L. Dennany, M. Gerlach, S. O'Carroll, T. E. R. J. Forster and P. Bertoncello, *J. Mater. Chem.*, 2011, **21**, 13984–13990.
6 L. Hu and G. Xu, *Chem. Soc. Rev.*, 2010, **39**, 3275–3304.
7 A. W. Knight and G. M. Greenway, *Analyst*, 1994, **119**, 879–890.
8 P. Bertoncello and R. J. Forster, *Biosens. Bioelectron.*, 2009, **24**, 3191–3200.
9 J. K. Lee, D. S. Yoo, E. S. Handy and M. F. Rubner, *Appl. Phys. Lett.*, 1996, **69**, 1686–1688.
10 W. K. Ward, *ASAIO J.*, 1999, **45**, 555–561.
11 A. Weisner, *Curr. Pharm. Biotechnol.*, 2004, **5**, 45–67.
12 M. S. Wilson, *Anal. Chem.*, 2005, **77**, 1496–1502.
13 A. E. Cass, G. Davis, G. D. Francis, H. A. O. Hill, W. J. Aston, J. Higgins, E. V. Plotkin, L. D. L. Scott and P. F. Tuner, *Anal. Chem.*, 1984, **56**, 667–671.
14 L. Dennany, E. J. O'Reilly, P. C. Innis, G. G. Wallace and R. J. Forster, *J. Phys. Chem. B*, 2008, **112**, 12907–12912.
15 O. Haas, M. Kierns and J. G. Vos, *J. Am. Chem. Soc.*, 1981, **103**, 1318–1319.
16 P. Qu, D. W. Thompson and G. J. Meyer, *Langmuir*, 2000, **16**, 4662–4671.
17 R. P. Swager, *J. Am. Chem. Soc.*, 1999, **121**, 1100–1104.
18 E. Rampazzo, S. Bonacchi, D. Genovese, J. Riccardo, M. Marcaccio, M. Montalti, F. Paolucci, M. Sgarzi, G. Valenti, N. Zaccheroni and L. Prodi, *Coord. Chem. Rev.*, 2012, **256**, 1664–1681.
19 W. Miao, *Chem. Rev.*, 2008, **108**, 2506–2553.
20 A. L. Kanibolotsky, F. Vilela, J. C. Forgie, S. E. T. Elmasly, P. J. Skabara, K. Zhang, B. Tieke, J. McGurk, C. R. Belton, P. N. Stavrinou and C. D. D. Bradley, *Adv. Mater.*, 2011, **23**, 2093–2097.
21 C. G. Cameron and P. G. Pickup, *J. Am. Chem. Soc.*, 1999, **121**, 11772–11779.
22 C. R. Belton, A. L. Kanibolotsky, J. Kirkpatrick, C. Orofini, S. E. T. Elmasly, P. N. Stavrinou, P. J. Skabara and D. D. C. Bradley, *Adv. Funct. Mater.*, 2013, **23**, 2792–2804.
23 E. J. O'Reilly, L. Dennany, D. Griffith, F. Moser, T. E. Keyes and R. J. Forster, *Phys. Chem. Chem. Phys.*, 2011, **13**, 7095–7101.
24 L. Dennany, T. E. Keyes and R. J. Forster, *Analyst*, 2008, **133**, 753–759.
25 L. Dennany, E. J. O'Reilly, P. C. Innis, G. G. Wallace and R. J. Forster, *Electrochim. Acta*, 2008, **53**, 4599–4605.
26 K. M. Omer, A. L. Kanibolotsky, P. J. Skabara, I. F. Perepichka and A. J. Bard, *J. Phys. Chem. B*, 2007, **111**, 6612–6619.
27 A. Venkatanarayanan, A.-M. Spehar-Délèze, L. Dennany, Y. Pellegrin, T. E. Keyes and R. J. Forster, *Langmuir*, 2008, **24**(19), 11233–11238.
28 E. J. O'Reilly, T. E. Keyes, R. J. Forster and L. Dennany, *Analyst*, 2013, **138**(2), 677–682.